Materials Research Proceedings 44 (2024) 708-717 https://doi.org/10.21741/9781644903254-76

α'-martensite grading techniques in reverse flow forming of AISI 304L

ARIAN Bahman[1,a *], HOMBERG Werner[1], KERSTING Lukas[2,b], TRÄCHTLER Ansgar[2], ROZO VASQUEZ Julian[3,c] and WALTHER Frank[3]

[1]Paderborn University, Forming and Machining Technology (LUF), Germany

[2]Fraunhofer Institute for Mechatronic Systems Design (IEM), Germany

[3]TU Dortmund University, Chair of Materials Test Engineering (WPT), Germany

[a]ba@luf.upb.de, [b]lukas.kersting@iem.fraunhofer.de, [c]julian.rozo@tu-dortmund.de

Keywords: Reverse Flow Forming, α'-Martensite, Grading Strategies, Property-Control

Abstract. Manufacturing processes benefit from property-control enabling reproducibility, application-oriented outcomes, and efficient part production. In reverse flow forming, state-of-the-art practices focus primarily on geometry-control, neglecting property-control. Given the intricacies of the process involving the interaction of tool and machine behavior, process parameters, properties of semi-finished products and temperatures, incorporating process-control becomes an imperative for producing components with predefined properties. The property controlled within this reverse flow forming process is the local α'-martensite content. Therefore, process strategies to actively influence the α'-martensite content must be implemented. In this study seamless AISI 304L steel tubes are used, where α'-martensite formation is strain- and/or temperature-induced through phase transformation within the process. This paper presents innovative process strategies, methods, and specially developed mechanical and thermal actuator systems to locally increase or suppress the α'-martensite content. The use and implementation of these approaches and tools allows the creation of unique optically invisible microstructure profiles containing 3D-gradings, implying a radial grading of α'-martensite. The locally implemented α'-martensite, forming these 3D-gradings, offers potential applications for functional or sensory purposes. This paper extends beyond theoretical concepts, providing tangible component outcomes.

Introduction

Flow formed tubes, exemplifying outstanding surface quality and precise dimensional accuracy, find widespread application in the automotive and aerospace industries [1]. Besides the visible effects on components, metal forming processes have a profound effect on the microstructure of formed parts [2]. The resulting properties of components in forming processes are an outcome of the collective influence of input parameters, such as the selected process parameters of the forming machine or the choice of the semi-finished material, along with the concurrent process variables that prevail during the deformation, including factors like the temperature within the forming zone and the applied forming forces. Thus, significant property-control within flow forming, which is not yet state of the art, requires the ability to control both, process parameters like the feed rate or the infeed as well as the forming temperature. This is particularly crucial when using TRIP steels such as AISI 304L, where phase transformation from austenite to α'-martensite is strain- and/or temperature-induced [3]. Although achieving geometrical reproducibility in flow formed AISI 304L parts is feasible, each produced component exhibits an arbitrary three-dimensional microstructure profile, indicating a corresponding arbitrary distribution of α'-martensite. A promising approach for the production of flow formed parts with defined geometry and property is closed-loop property-control. Numerous experiments were carried out as part of a priority program funded by the DFG, aiming for the development of innovative process strategies to

successfully produce flow formed parts with locally enhanced or reduced α'-martensite contents. These grading techniques can then be used to create invisible microstructure profiles, in the sense of an invisible "barcode", within the forming process of the tubes. This proposes a pioneering method for achieving tamper-proof part production in reverse flow forming, requiring inventive measurement concepts, as the fundamental aspect of property-control involves observing the pertinent properties or their associated system states [4]. Hence, a softsensor has been devised and implemented within the flow forming process to detect local variations in magnetic component properties and to correlate these with the estimated α'-martensite content [5]. The measurement concept also includes a laser system that ensures the component geometry by monitoring plastic deformation and provides real-time information to the control system. Building upon the accomplished local grading and control of α'-martensite in axial (1D) and axial-angular (2D) directions through solely mechanical or thermomechanical process strategies, this paper advances further by presenting innovative and intricate approaches for achieving α'-martensite grading in radial direction (3D). The aim is to experimentally validate whether the indention depth of the α'-martensite can be influenced by thermal actuators and/or mechanical forming strategies, for example by generating radial temperature gradients or varying the number of flow forming passes. In Fig. 1, various grading types are showcased through a color-coded tube. The red color highlights the 3D-grading, the primary focus of this study, with the radial direction representing the thickness of the tube.

Fig. 1. Differentiation of grading types.

Reverse Flow Forming

The incremental process of flow forming offers in particular significant advantages in flexibility and efficiency [6]. A key feature of flow forming is the intentional reduction in wall thickness Δw of semi-finished tubes. This reduction results in a component elongation Δl caused by volume constancy, accompanied by excellent shape, dimensional accuracy and superior surface qualities [7]. Flow formed tubes adhere to stringent standards, particularly those established by the aerospace industry, and find widespread application in high-performance components such as drive shafts for jet engines and helicopters [8]. This paper focuses on reverse flow forming, as illustrated in Fig. 2, where the material flow occurs counter to the axial motion of the roller tools. These versatile roller tools, capable of both axial and radial movement, rotate around their own axis due to contact friction with the rotating tube.

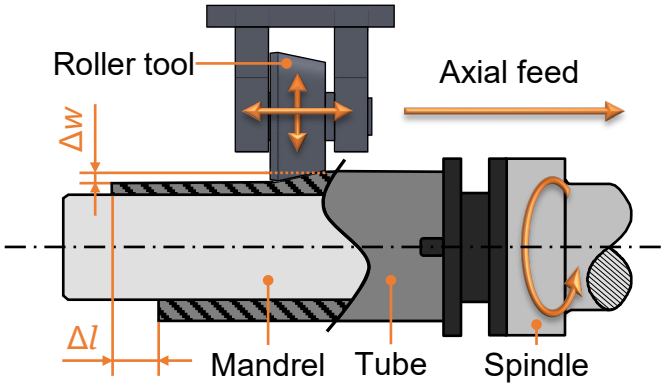

Fig. 2. Reverse flow forming process principle.

Experimental Setup

All the experiments for the study were carried out on a PLB 400 spinning machine from Leifeld Metal Spinning GmbH (Ahlen, Germany) with a drive power reaching up to 11 kW and a maximum spindle speed of 950 rpm. The forming machine is equipped with a hydraulically driven cross support, featuring two machining axes custom-developed at Forming and Machining Technology (LUF) in Paderborn University. Each axis (X/Y-axis) can generate a maximum force of 35 kN. The experimental setup, depicted in Fig. 3, incorporates a single-roller tool configuration, crucial to create sufficient space to accommodate thermal actuator systems and sensors dedicated to process control.

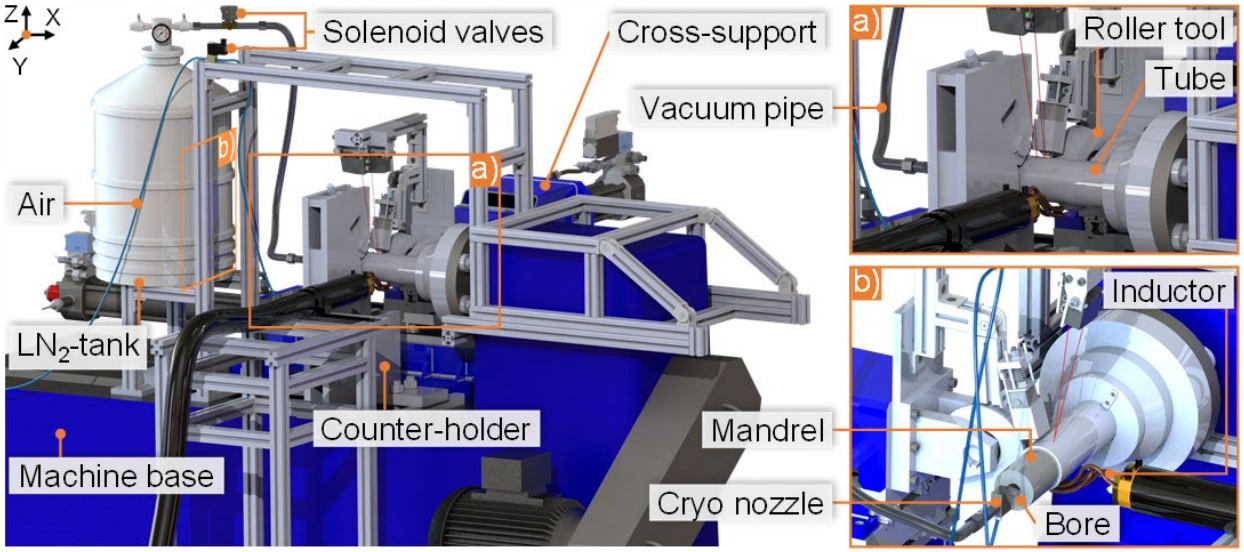

Fig. 3. Machine and actuator configuration with a) and b) showing different viewing angles.

Initially introduced in [9] and later optimized in [10], the sensor concept developed at Forming and Machining Technology (LUF) will not be the primary focus of this work. Moreover, the setup includes a robust counter-holder specifically designed to support the mandrel, along with an absolute value encoder enabling angle-dependent operations within the process. The thermal heating actuator comprises a custom-developed inductor that conforms to the shape of the semi-finished tube, allowing for localized heating in a specific angular area. In addition to the thermal heating actuator, the setup also includes its counterpart, a thermal cooling actuator. The custom-developed automated cryogenic system (Fig. 4) can be used for global or local cooling.

Materials Research Proceedings 44 (2024) 708-717 https://doi.org/10.21741/9781644903254-76

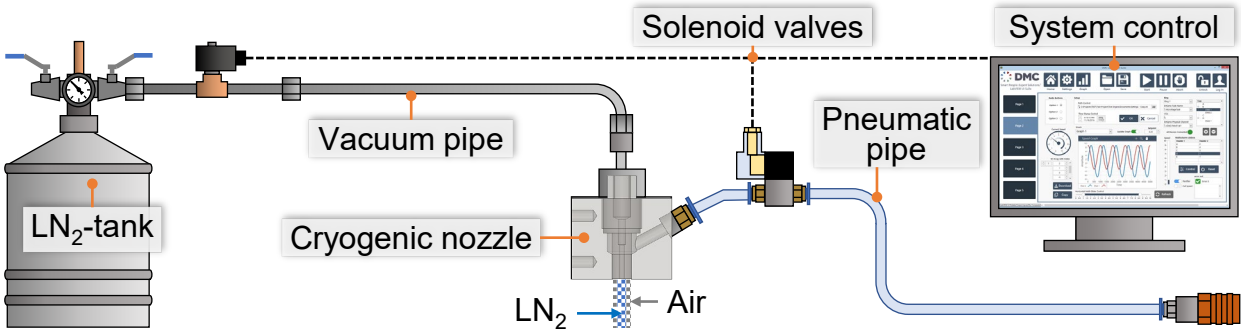

Fig. 4. Automated cryogenic cooling system.

Previously detailed in [11], it includes a liquid nitrogen tank, a flexible stainless steel vacuum pipe, pneumatic pipes, a set of solenoid valves and a two-component cryogenic nozzle bundling liquid nitrogen surrounded by compressed air. The use of solenoid valves, coupled with an absolute value encoder, enables automated and reproducible cooling through computer assistance. To achieve efficient cooling, the cryogenic nozzle focuses a stream of liquid nitrogen at a temperature of -196°C, which creates significant temperature gradients in a short period of time. Utilizing the nozzle allows for the atomization of liquid nitrogen, preventing the Leidenfrost phenomenon [12] that typically occurs when pouring liquid nitrogen in its liquid form. During the conducted experiments, a specially designed hollow mandrel with a diameter of 72 mm and a centric bore of 25 mm was employed. Despite its bore, the mandrel exhibits adequate stability and facilitates indirect cooling of the tube by cooling through the bore. Temperature measurements during the experiments were carried out using a set of tactile thermocouples, chosen for their superior reliability in comparison to optical methods, such as thermographic measurements. A spring-loaded thermocouple, positioned above the tube, measured its surface temperature in proximity to the forming zone (the contact area between the roller tool and the rotating tube). The second thermocouple was positioned inside the tube, between the mandrel, to measure the temperature of the tube's inner surface. Due to the rotation of both the tube and the mandrel, the second thermocouple could not be connected to a standard measuring device via cable. Consequently, a Bluetooth Mini Datalogger was integrated into the rotating spindle, enabling cable-free transmission of temperature values. The semi-finished material used for the experiments was AISI 304L (X2CrNi18-9, 1.4307), a TRIP steel with strain- and/or temperature-induced α'-martensite formation [13]. The detection method for α'-martensite included a precision measurement setup, featuring a Feritscope for reproducible results.

3D-Grading Strategies

The novel introduced grading strategies aim for 3D-graded structures with locally adjusted α'-martensite content useful for functional or sensory purposes in high-performance components.

Temperature gradient strategy. Controlling α'-martensite formation in the radial (thickness) direction of tubes encompasses the management of various factors, including temperature. To establish the desired temperature gradient, cryogenic cooling and induction heating with thermal actuators are employed. One thermal strategy involves combining tube induction heating with indirect mandrel cooling of its inner surface. Copper foil, acting as magnetic induction shielding, can be placed between the tube and mandrel to block heat transfer to the tube's interior and enhance the temperature gradient across the wall thickness (Fig. 5).

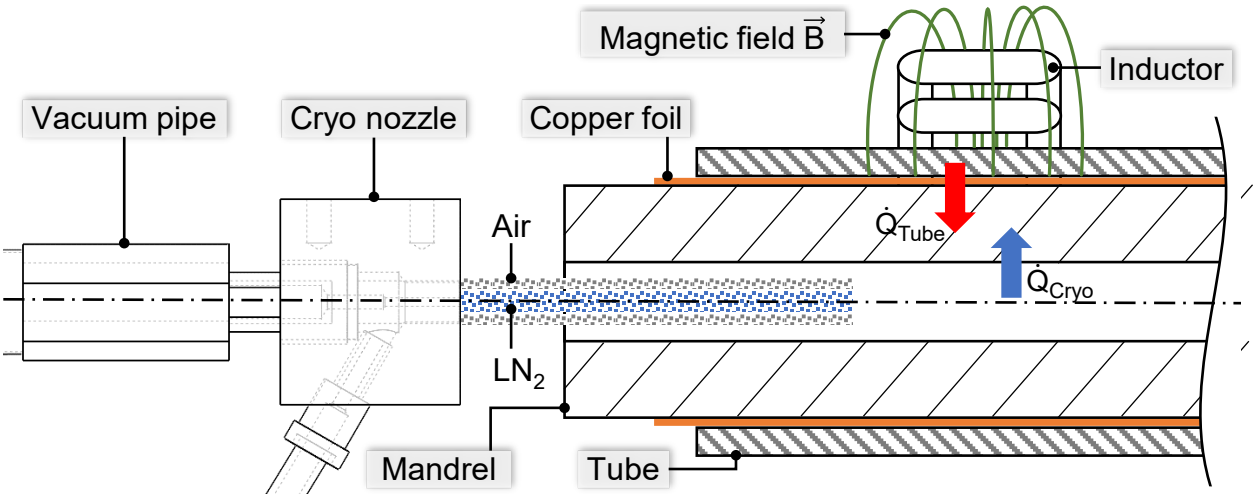

Fig. 5. Temperature gradient strategy: Combining induction heating and indirect cooling.

As previously described, the tube's inner surface cools indirectly through contact with the cooled mandrel. In isothermal flow forming, α'-martensite content peaks on the outer surface due to roller tool contact, gradually diminishing towards the inner surface. To counter this, cooling the inner surface and heating the outer surface during flow forming could normalize or even reverse α'-martensite formation in the radial direction.

Knead strategy. This isothermal knead strategy leverages the phenomenon of increased α'-martensite formation with successive passes for the same amount of wall thickness reduction. Whether inducing a 2 mm reduction in wall thickness with a single pass or with multiple passes in increments of e.g. 0.2 mm, yields significantly different α'-martensite content on the outer surface of the tube, as demonstrated in [14]. Further investigation is required to ascertain if this discrepancy extends to influence α'-martensite formation in the radial direction, potentially making it a viable strategy for influencing such formation.

Results and Discussion

For comparison purposes, a flow formed reference sample was produced isothermally, utilizing a 2 mm infeed (r), an axial feed rate of 0.1 mm/s (f), and a rotational speed of 30 rpm (n). The sample served to investigate the impact of thermal and kneading strategies on radial α'-martensite formation.

Temperature gradient strategy. Fig. 6, captured with the Smartzoom 5 automated digital microscope from ZEISS (Oberkochen, Germany), compares cross-sections of the reference sample in a) with samples produced via b) induction heating (tube surface temperature of 100°C) and c) cryogenic cooling (tube surface temperature of -40°C) using identical process parameters and wall thickness reductions. The microstructure comparison reveals that lower temperatures result in a higher concentration of α'-martensite needles (indicated by black areas), making the microstructure in c) appear darkest. Additionally, the concentration is observed to be highest at the surface, diminishing radially.

Materials Research Proceedings 44 (2024) 708-717 https://doi.org/10.21741/9781644903254-76

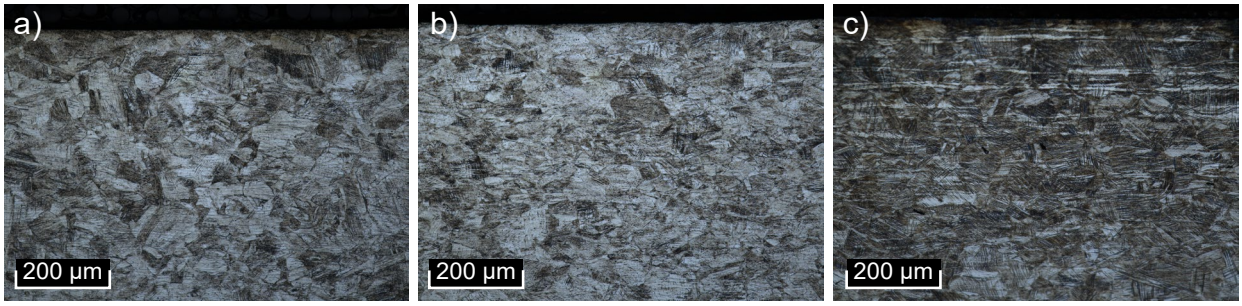

Fig. 6. Microscopic cross-sections: a) ref. sample, b) induction heating, c) cryogenic cooling.

As this type of evaluation is limited to a very localized area and only allows qualitative statements, the entire cross-section (Fig. 7 d) was measured precisely and reproducibly using a specially developed measurement setup. For this, a Feritscope was used measuring the α'-martensite content along the cross-section in the form of a grid with intervals of 0.375 mm/0.25 mm in the Y-(radial) direction and 3 mm in the X-direction (Fig. 7).

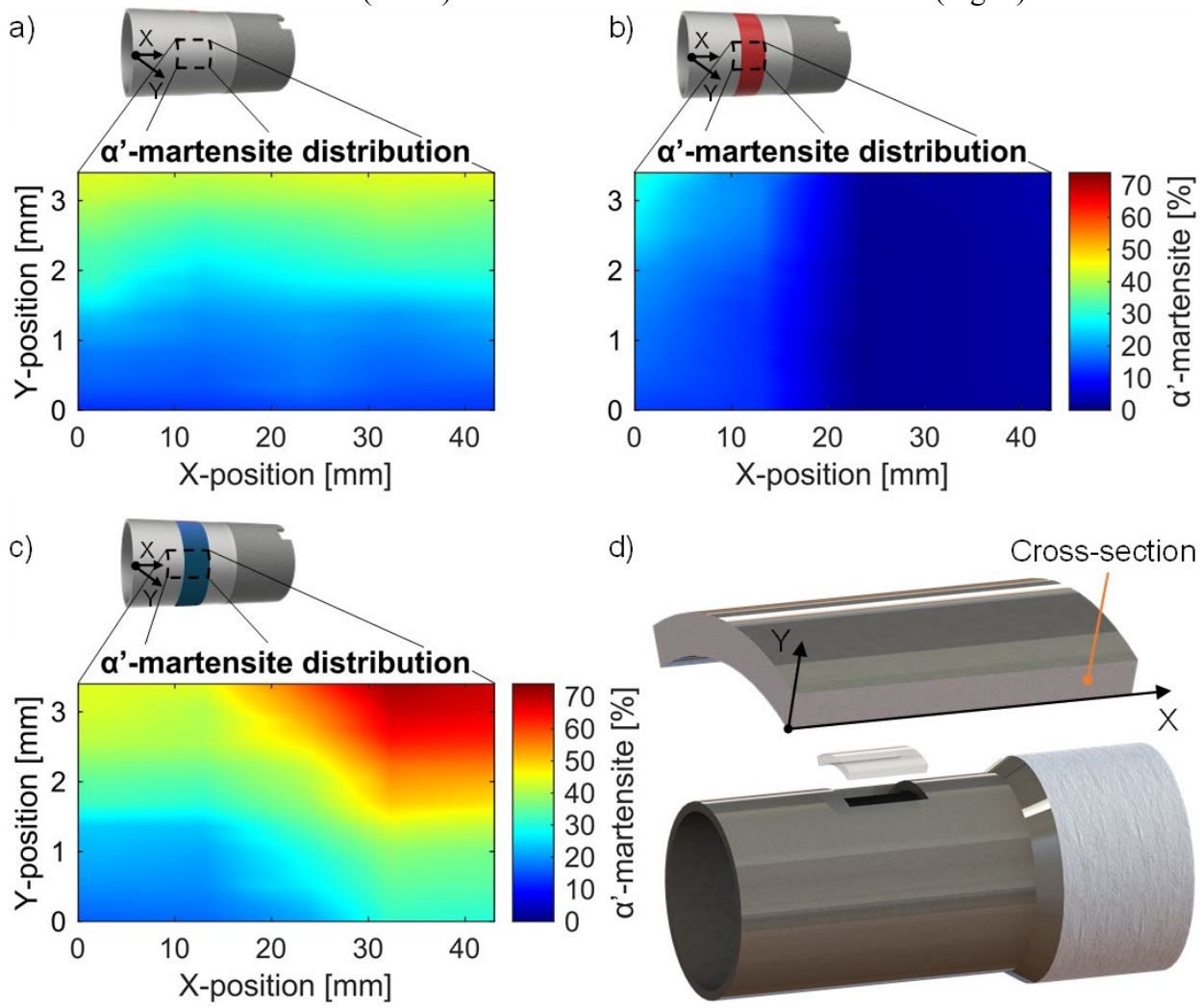

Fig. 7. Cross-section measurements: a) ref. sample, b) induction heating, c) cryogenic cooling, d) highlights the focused cross-section.

The measurements confirm the qualitative evaluation using microscopy. Additionally, cooling in Fig. 7 c) results in deeper penetration of α'-martensite formation compared to the reference sample in Fig. 7 a). The comparison of the grading resolution/sharpness between tempered and

non-tempered areas (transition area) shows significant differences between induction heating (Fig. 7 b) and cryogenic surface cooling (Fig. 7 c). Induction heating creates a vertical grading line in radial direction, indicating an abrupt temperature change. Cryogenic surface cooling results in a diagonal grading line and a transition length of approx. 20 mm, implying a gradual temperature change due to radial heat conduction dependency. The temperature gradient for cryogenic surface cooling amounted approx. 20 K ($T_{surface}$ ≈ -40°C, $T_{inner\ surface}$ ≈ -20°C) while for induction heating no temperature gradient was observed ($T_{surface}$ ≈ 100°C, $T_{inner\ surface}$ ≈ 100°C). Further experiments compared radial α'-martensite formation between direct surface cooling at -40°C (Fig. 8 b) and indirect cooling (Fig. 8 c) via the mandrel (with both tube surface and inner surface at -40°C), as illustrated in Fig. 8. Indirect cooling from the tube's interior results in greater depth and α'-martensite content compared to surface cooling. The deformation process during surface cooling heats deeper material layers reducing α'-martensite formation.

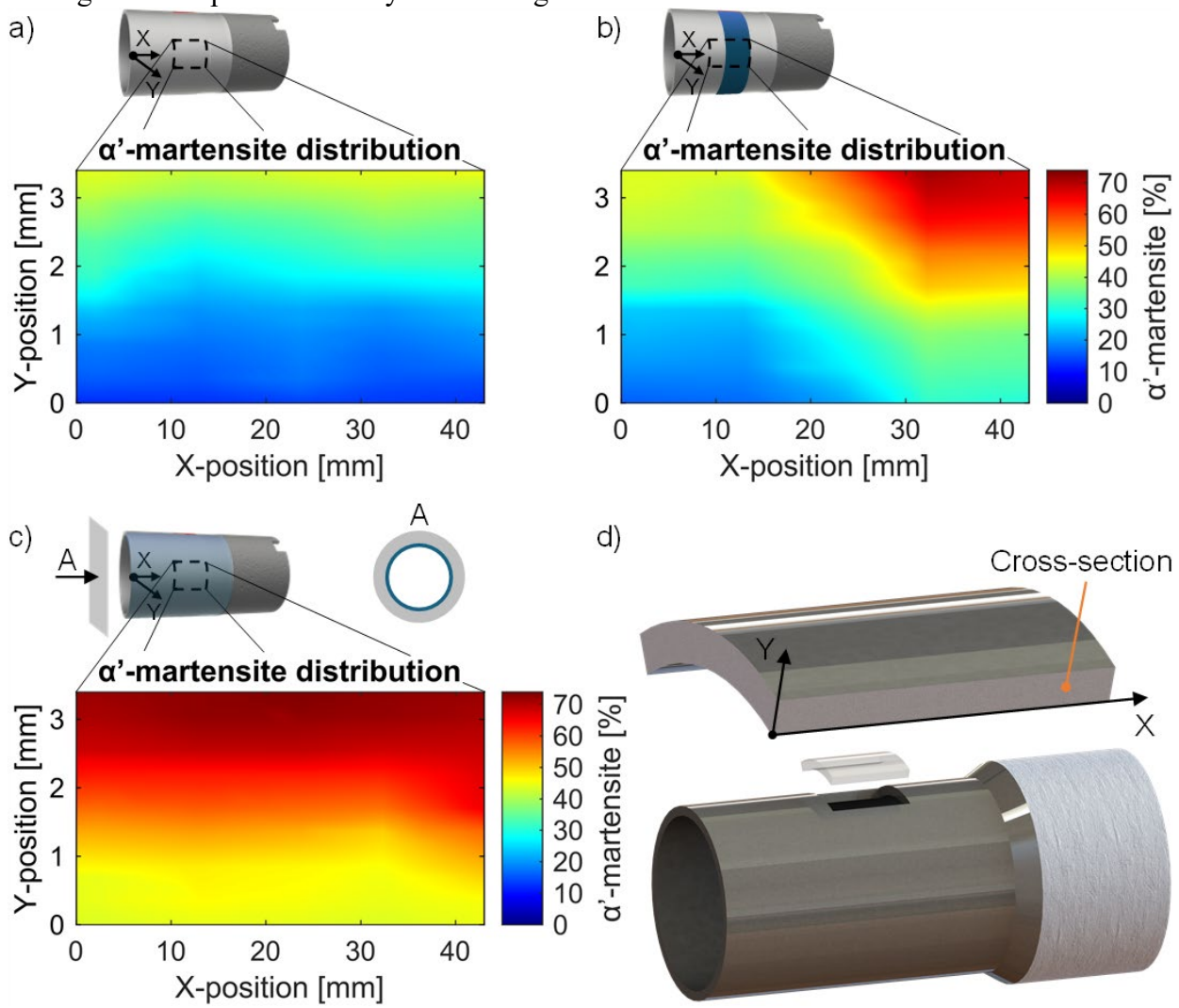

Fig. 8. Cross-section measurements: a) ref. sample, b) direct surface cooling, c) indirect cooling, d) highlights the focused cross-section.

The next strategy involves combining tube induction heating with indirect mandrel cooling of its inner surface, which was described in Fig. 5. Fig. 9 compares radial α'-martensite formation among the reference sample (Fig. 9 a), the combined heating and cooling strategy without (Fig. 9 b), and with copper foil (Fig. 9 c). Without copper foil, α'-martensite formation is completely suppressed, while its use effectively shields the magnetic field, keeping the mandrel cool and

Materials Research Proceedings 44 (2024) 708-717 https://doi.org/10.21741/9781644903254-76

preventing heating of the tube's interior. This leads to a homogenization of the α'-martensite content throughout the tube's wall thickness. The use of copper foil enables investigations of the grading resolution/sharpness of the transition area between indirectly cooled and cooled as well as heated areas. The result is a diagonal grading line and a transition length of approx. 13 mm, implying a gradual temperature change. The max. temperature gradient for the combined indirect cryogenic cooling and induction heating amounted approx. 50 K ($T_{surface}$ ≈ 25°C, $T_{inner\ surface}$ ≈ -25°C).

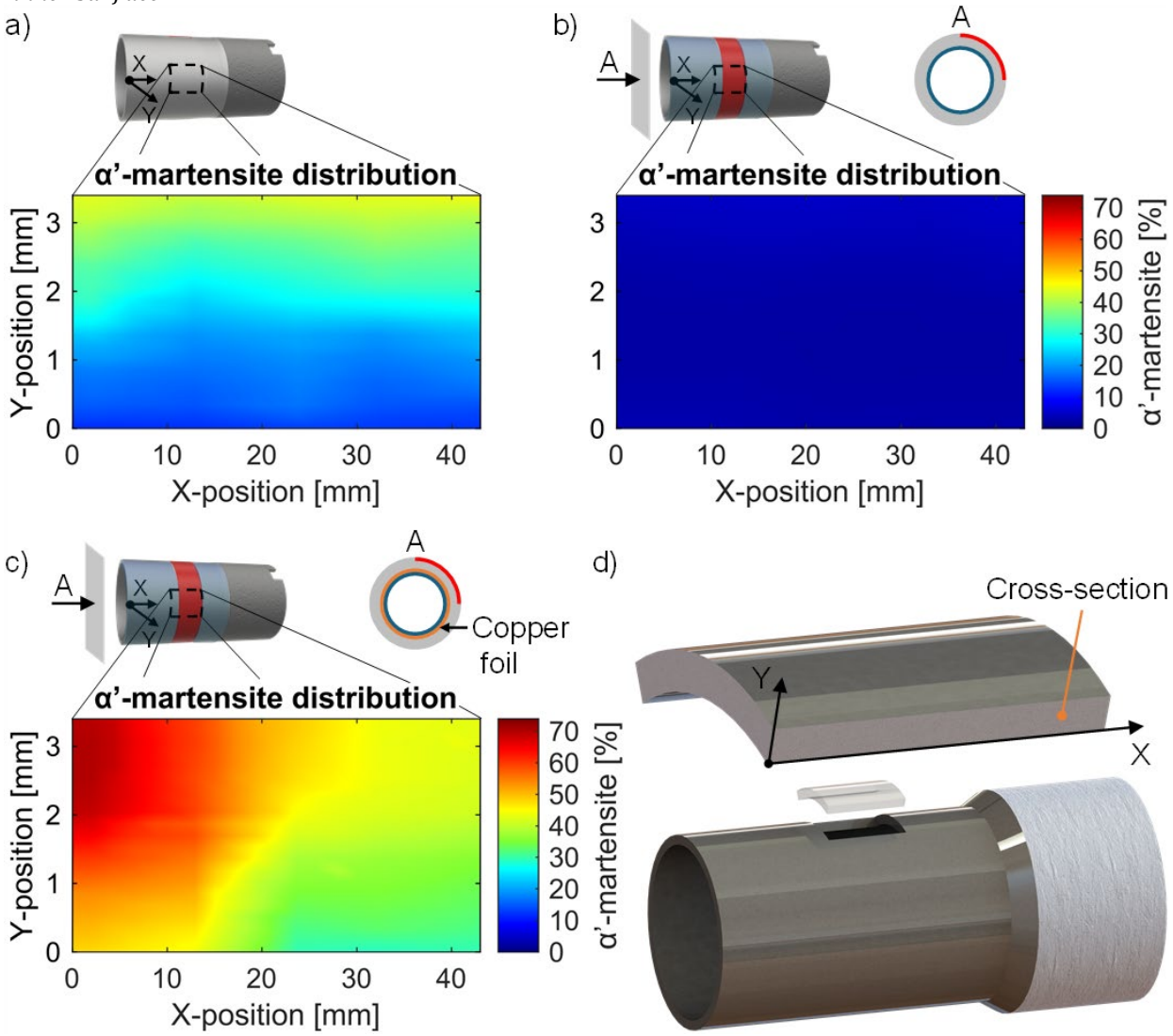

Fig. 9. Cross-section measurements: a) ref. sample, combination of indirect cooling and induction heating in b) without and c) with copper foil, d) highlights the focused cross-section.

Knead strategy. This isothermal strategy uses the number of passes instead of temperature to affect the α'-martensite content. Fig. 10 compares the cross-section of two samples with a wall thickness reduction of 2 mm each. Fig. 10 a) depicts radial α'-martensite distribution for five passes using a 2 mm infeed (*r*). In contrast, Fig. 10 b) shows the distribution of α'-martensite resulting from five passes using a 1 mm infeed followed by four passes with 2 mm. The comparison demonstrates that the radial distribution of α'-martensite is influenced by the number of passes. More passes yield increased depth and higher, more homogenized concentration of α'-martensite for the same 2 mm wall thickness reduction, making the Knead strategy suitable for 3D-grading.

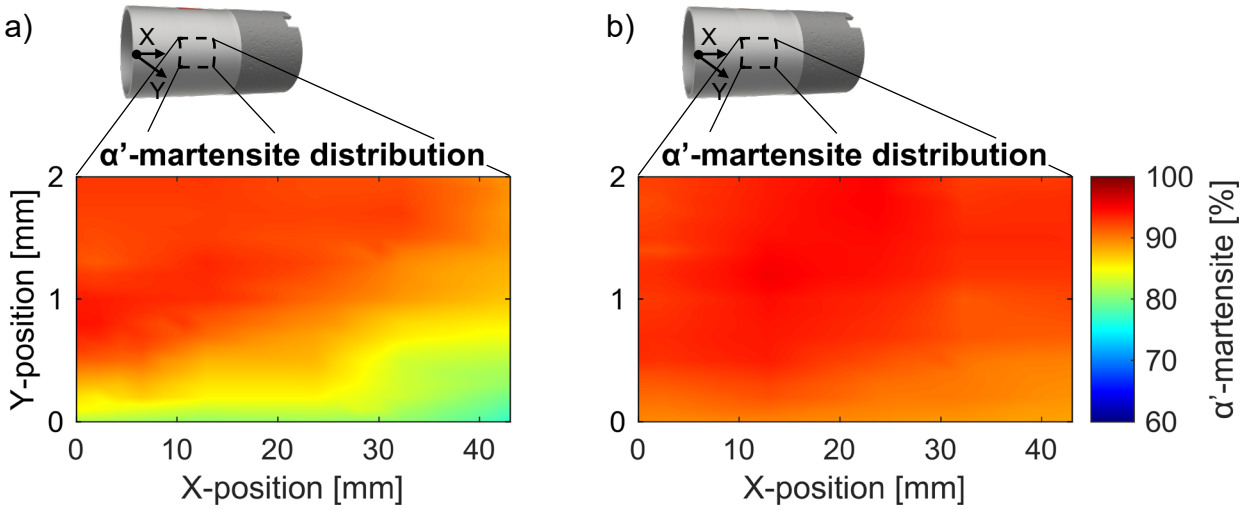

Fig. 10. Cross-section measurements: 2 mm thickness reduction with a) five passes and r = 2 mm, b) five passes and r = 1 mm followed by four passes and r = 2 mm.

Conclusions and Outlook

In this study, innovative strategies for 3D-grading in reverse flow forming have been demonstrated, notably the "Temperature gradient strategy" and the isothermal "Knead strategy". These strategies have demonstrated remarkable effectiveness in influencing the α'-martensite formation and distribution in radial direction over the thickness of tubes, while maintaining constant wall thickness reduction. The "Temperature gradient strategy", leveraging specially developed cryogenic and induction heating systems, proved instrumental in creating controlled temperature gradients during the reverse flow forming process. Of particular significance is the integration of induction heating alongside indirect cooling, augmented by the strategic application of copper foil to neutralize undesired magnetic field induction. This refined method not only facilitates temperature management but also empowers manipulation of α'-martensite formation and distribution in radial direction. Furthermore, it promotes deeper penetration of α'-martensite formation and addresses inherent inhomogeneities typically observed in conventional flow forming processes by homogenizing α'-martensite distribution. Furthermore, the isothermal "Knead strategy" showcased the potential for manipulating α'-martensite distribution through variations in flow forming passes. These innovative approaches offer precise control over microstructural features, promising advancements in material processing and component manufacturing, with potential applications in automotive and aerospace industries.

Acknowledgements

The authors would like to thank the German Research Foundation (Deutsche Forschungsgemeinschaft, DFG) for their support of the depicted research within the priority program SPP 2183 "Property controlled deformation processes", through project no. 424335026 "Property control during spinning of metastable austenites".

References

[1] M. Haridas, G. Gopal, A. Ramesh, R.K. Katta, Modelling and simulation of single and multi-pass flow forming to investigate the influence of process parameters on part accuracy, IJMR 11 (2016) 79473. https://doi.org/10.1504/IJMR.2016.079473

[2] D.A. Hughes, N. Hansen, The microstructural origin of work hardening stages, Acta Mater. 148 (2018) 374–383. https://doi.org/10.1016/j.actamat.2018.02.002

[3] A. Weidner, Deformation Processes in TRIP/TWIP Steels (295). Cham: Springer International Publishing, 2020.

[4] M. Bambach, T. Meurer, W. Homberg, S. Duncan, Editorial to special issue “Property-controlled forming processes”, 2022. https://doi.org/10.3929/ethz-b-000530958

[5] W. Homberg, B. Arian, V. Arne, T. Borgert, A. Brosius, P. Groche, C. Hartmann, L. Kersting, R. Laue, J. Martschin, T. Meurer, D. Spies, A.E. Tekkaya, A. Trächtler, W. Volk, F. Wendler, M. Wrobel, Softsensors: key component of property control in forming technology, Prod. Eng. Res. Devel. 18 (2023) 603-614. https://doi.org/10.1007/s11740-023-01227-1

[6] M. Runge, Spinning and Flow forming: spinning and flow forming technology, product design, equipment, control systems. Landsberg/Lech: Moderne Industrie, 1994.

[7] M. Sivanandini, S.S. Dhami, B.S. Pabla, Flow forming of tubes-A review, Int. J. Sci. Eng. Res. 3 (2012) Art. no. 5. [Online]. Available: https://www.ijser.org/researchpaper/Flow-Forming-Of-Tubes-A-Review.pdf

[8] J. Savoie, M. Bissinger, Case studies and applications of flow forming to aircraft engine component manufacturing, KEM 344 (2007) 443–450. https://doi.org/10.4028/www.scientific.net/KEM.344.443

[9] M. Riepold, B. Arian, J. Rozo Vasquez, W. Homberg, F. Walther, A. Trächtler, Model approaches for closed-loop property control for flow forming, Adv. Industr. Manuf. Eng. 3 (2021) 100057. https://doi.org/10.1016/j.aime.2021.100057

[10] B. Arian, W. Homberg, L. Kersting, A. Trächtler, J. Rozo Vasquez, F. Walther, Produktkennzeichnung durch lokal definierte Einstellung von ferromagnetischen Eigenschaften beim Drückwalzen von metastabilen Stahlwerkstoffen: Ideen Form geben: 36. Aachener Stahlkolloquium Umformtechnik: 26.-27. Oktober 2022, Eurogress Aachen: Tagungsband, 1st ed. Aachen: Verlagshaus Mainz GmbH, 2022.

[11] B. Arian, W. Homberg, J. Rozo Vasquez, F. Walther, L. Kersting, A. Trächtler, Cryogenic reverse flow forming of AISI 304L, Mater. Res. Forum LLC (2023). https://doi.org/10.21741/9781644902479-219

[12] Y. Guo, X. Liu, J. Ji, Z. Wang, X. Hu, Y. Zhu, T. Zhang, T. Tao, K. Liu, Y. Jiao, Delayed leidenfrost effect of a cutting droplet on a microgrooved tool surface, Langmuir: the ACS journal of surfaces and colloids, early access. https://doi.org/10.1021/acs.langmuir.3c00592

[13] M. Jambor, T. Vojtek, P. Pokorný, M. Šmíd, Effect of solution annealing on fatigue crack propagation in the AISI 304L TRIP steel, Materials, early access. https://doi.org/10.3390/ma14061331

[14] B. Arian, W. Homberg, J. Rozo Vasquez, F. Walther, M. Riepold, A. Trächtler, Forming of metastable austenitic stainless steel tubes with axially graded martensite content by flow-forming, ESAFORM 2021, 2021. https://doi.org/10.25518/esaform21.2759